

STRUCTURAL ADHESIVES:

Developments in Resins and Primers

A. J. KINLOCH

STRUCTURAL ADHESIVES:

Developments in Resins and Primers

Edited by

A. J. KINLOCH

*Department of Mechanical Engineering,
Imperial College of Science and Technology,
London, UK*

ELSEVIER APPLIED SCIENCE PUBLISHERS
LONDON and NEW YORK

ELSEVIER APPLIED SCIENCE PUBLISHERS LTD
Crown House, Linton Road, Barking, Essex IG11 8JU, England

Sole Distributor in the USA and Canada
ELSEVIER SCIENCE PUBLISHING CO., INC.
52 Vanderbilt Avenue, New York, NY 10017, USA

WITH 44 TABLES AND 135 ILLUSTRATIONS

© ELSEVIER APPLIED SCIENCE PUBLISHERS LTD 1986

British Library Cataloguing in Publication Data

Structural adhesives: developments in resins
and primers.

1. Building materials 2. Adhesives

I. Kinloch, A. J.

691'.99 TA455.A34

Library of Congress Cataloging in Publication Data

Structural adhesives.

Bibliography: p.

Includes index.

1. Adhesives. I. Kinloch, A. J.

TP968.S84 1986 668'.37 86-6340

ISBN 1-85166-002-X

The selection and presentation of material and the opinions expressed in this publication
are the sole responsibility of the authors concerned

Special regulations for readers in the USA

This publication has been registered with the Copyright Clearance Center Inc. (CCC),
Salem, Massachusetts. Information can be obtained from the CCC about conditions
under which photocopies of parts of this publication may be made in the USA. All other
copyright questions, including photocopying outside of the USA, should be referred to
the publisher.

All rights reserved. No part of this publication may be reproduced, stored in a retrieval
system, or transmitted in any form or by any means, electronic, mechanical, photocopy-
ing, recording or otherwise, without the prior written permission of the publisher.

Typeset and printed at The Universities Press (Belfast) Ltd

Preface

The use of adhesives in general industry continues to develop at a rapid pace and this is particularly the case for structural adhesives. Such adhesives are based upon resin compositions that polymerise to give high-modulus, high-strength adhesives so that a load-bearing joint is formed. As might be expected, developments in the chemistry and properties of structural adhesives have led and supported the spread of these materials from the high-technology aerospace industries into all types of general engineering applications. It appeared therefore to be an appropriate time to review some of the developments in our understanding of the chemistry, structure and properties of resins which are used in the technology of structural adhesives bonding.

The resins which form the mainstay of the industry are the epoxies and acrylics and several chapters consider various aspects of these materials. In Chapter 1 the effect of cure conditions on the final properties of the resin are discussed and this chapter extends the most useful concepts of time-temperature-transformation diagrams to rubber-toughened epoxy resins. In the next two chapters authors from two of the world's leading adhesives companies review recent developments in acrylic- and epoxy-based adhesives. In Chapter 4 the comparatively new bismaleimide resins are discussed. These materials possess relatively high thermal resistance but are readily processable and, since they are new materials, their use as matrix materials in fibre composites as well as in structural adhesives is considered. Structural adhesive formulations usually contain additives such as rubbers and

rigid-particulate fillers and Chapters 5 and 6 review the relationships between the microstructure and properties of such materials. In the next chapter the contentious issue of whether there is a definite microstructure in simple epoxy resins is addressed, and whether any microstructure would affect the properties of the material. Finally, in adhesives technology the problem of attaining good resistance to moisture for the bonded assembly always represents a challenge and the use of silane resin coupling agents to achieve this goal is increasing. Thus, the book concludes with a review chapter on this important area in adhesives technology.

A. J. KINLOCH

Contents

<i>Preface</i>	v
<i>List of Contributors</i>	xi
Chapter 1 Cure and Properties of Thermosetting Polymers . .	1
J. K. GILLHAM	
1 The Time-Temperature-Transformation Cure Diagram and Properties of Thermosetting Systems	1
2 Torsional Braid Analysis/Torsion Pendulum: A Technique for Characterizing Thermosetting Systems	6
3 Rubber-Modified Epoxies: Cure, Transitions, Morphology and Mechanical Properties	12
3.1 Introduction	12
3.2 Materials	14
3.3 Torsional braid analysis (TBA) and the TTT cure diagram	16
3.4 Phase-separated versus dissolved rubber	18
3.5 Shear modulus versus temperature	22
3.6 Fracture behavior	23
4 Conclusions	26
Acknowledgement	26
References	27
Chapter 2 Acrylic-Based Adhesives	29
F. R. MARTIN	
1 Introduction	29
2 Chemistry of Acrylics	30

2.1	Cyanoacrylates	31
2.2	Methacrylates and acrylates	32
3	Adhesives—Developments	33
3.1	Cyanoacrylates	34
3.2	Anaerobics	39
3.3	Modified acrylic adhesives	41
4	Conclusion	52
	References	53
Chapter 3 Epoxy-Based Adhesives		57
E. W. GARNISH		
1	Introduction	57
2	Resins	57
3	Hardeners	60
3.1	Amine-based hardeners	60
3.2	Latent hardeners	63
3.3	Miscellaneous hardeners	65
4	Co-Reacting Compositions	67
5	Morphology	68
6	Modifying Constituents	69
7	Concluding Remarks	71
	References	72
Chapter 4 Bismaleimide Resins		77
H. STENZENBERGER		
1	Introduction	77
2	Synthesis of Bismaleimides	78
2.1	Difunctional monomaleimides (AB monomers)	81
3	Reactivity of Bismaleimides	82
3.1	Thermal homopolymerization	84
3.2	Radical-type homo- and copolymerization	84
3.3	Ionic-type homo- and copolymerization	87
3.4	Diene-type copolymerization	90
3.5	'Ene'-type linear chain extension copolymerization	91
3.6	Michael Addition copolymerization	92
3.7	Other co-monomers	95
4	Commercial Bismaleimides and Bismaleimide Resins	95
4.1	Compimide 353	96
4.2	Michael Addition resins	96
4.3	The XU 292 resin concept	105
4.4	The bismaleimide/cyanate resin concept	106
5	Commercial Prepreg Systems	109
6	Adhesives Based on Bismaleimide Resins	116
6.1	New toughened bismaleimide adhesives	119
7	Future Bismaleimide Development Requirements	123
	References	123

Chapter 5 Rubber-Toughened Thermosetting Polymers 127**A. J. KINLOCH**

	Notation	127
1	Introduction	127
2	Chemistry/Microstructure Relationships	131
2.1	Introduction	131
2.2	Chemical and physical properties of the rubber	131
2.3	Chemical and physical properties of resin/hardener	138
2.4	Time and temperature of cure	140
3	Microstructure/Mechanical Property Relationships	141
3.1	Introduction	141
3.2	Toughening mechanisms	142
3.3	Microstructural features of the matrix phase	150
3.4	Microstructural features of the rubbery phase	155
4	Concluding Remarks	160
	Acknowledgements	160
	References	161

Chapter 6 Rigid-Particulate Reinforced Thermosetting Polymers 163**R. J. YOUNG**

	Notation	163
1	Introduction	164
2	Structure	165
2.1	Fabrication	165
2.2	Characterisation	165
3	Deformation	168
3.1	Elastic deformation	168
3.2	Plastic deformation	171
4	Fracture	173
4.1	Fracture strength	173
4.2	Impact, fatigue and time-dependent failure	175
5	Crack Propagation	177
5.1	Particle volume fraction and size	179
5.2	Particle/matrix adhesion	180
5.3	Matrix toughness	182
5.4	Rate and temperature	184
6	Toughening Mechanisms	185
6.1	Crack pinning	185
6.2	Analysis of pinning	188
6.3	Crack opening displacement	192
6.4	Localised plastic deformation	194
7	Concluding Remarks	198
	Acknowledgements	198
	References	198

Chapter 7 Microstructure in Crosslinked Epoxy Polymers . . . 201

G. C. STEVENS

	Notation	201
1	Introduction	202
2	Networks Formation	203
2.1	Typical materials and reaction mechanisms	203
2.2	Ideal and non-ideal networks	210
2.3	Observed reaction behaviour	213
2.4	Uneven curing	220
3	Bulk microstructure	221
3.1	Microstructure in linear amorphous polymers	222
3.2	Scattering observations of inhomogeneity	222
3.3	Microscopy of bulk and surface structure	245
4	Relationships Between Physical Properties and Microstructure	251
4.1	Correlations during reaction	251
4.2	Influence on mechanical properties	255
4.3	Other properties and considerations	260
5	Concluding Remarks	260
	Acknowledgements	263
	References	263

Chapter 8 Silane Coupling Agents 269

J. COMYN

1	Introduction	269
2	Improvements in Bonding with Coupling Agents	273
3	Interaction of Silanes with Glass and Related Materials	275
4	Interaction of Silanes with Metals	288
5	Interactions of Functional Groups with Polymers and Resins	303
6	Titanate and Zirconate Coupling Agents	306
7	Concluding Remarks	308
	References	309

<i>Author Index</i>	313
-------------------------------	-----

<i>Subject Index</i>	323
--------------------------------	-----

Cure and Properties of Thermosetting Polymers

J. K. GILLHAM

*Polymer Materials Program,
Department of Chemical Engineering,
Princeton University,
New Jersey, USA*

1. THE TIME-TEMPERATURE-TRANSFORMATION CURE DIAGRAM AND PROPERTIES OF THERMOSETTING SYSTEMS

A time-temperature-transformation (TTT) cure diagram may be used to provide an intellectual framework for understanding and comparing the cure and physical properties of thermosetting systems.¹⁻¹⁰ The main features of an isothermal TTT cure diagram such as that shown in Fig. 1 can be obtained by measuring the times to events which occur during isothermal cure vs temperature (T_{cure}). These events include the onset of phase separation, gelation, vitrification, full cure, and devitrification. Gelation corresponds to the incipient formation of an infinite molecular network which gives rise to viscoelastic behavior in the macroscopic fluid. Vitrification occurs when the glass transition temperature rises to the isothermal temperature of cure. Devitrification occurs when the glass transition temperature decreases through the isothermal temperature (as in degradation). The diagram displays the distinct states encountered on cure due to chemical reactions. These states include liquid, sol/gel rubber, elastomer, ungelled (sol) glass, gelled glass, and char. The gelled glass region in the TTT cure diagram is divided into two parts by the full cure line:⁸ in the absence of degradation (Fig. 1, devitrification and char), the top and lower parts could be designated fully cured (gel) glass and undercured (sol/gel) glass region, respectively. The terms A-, B- and C-stage

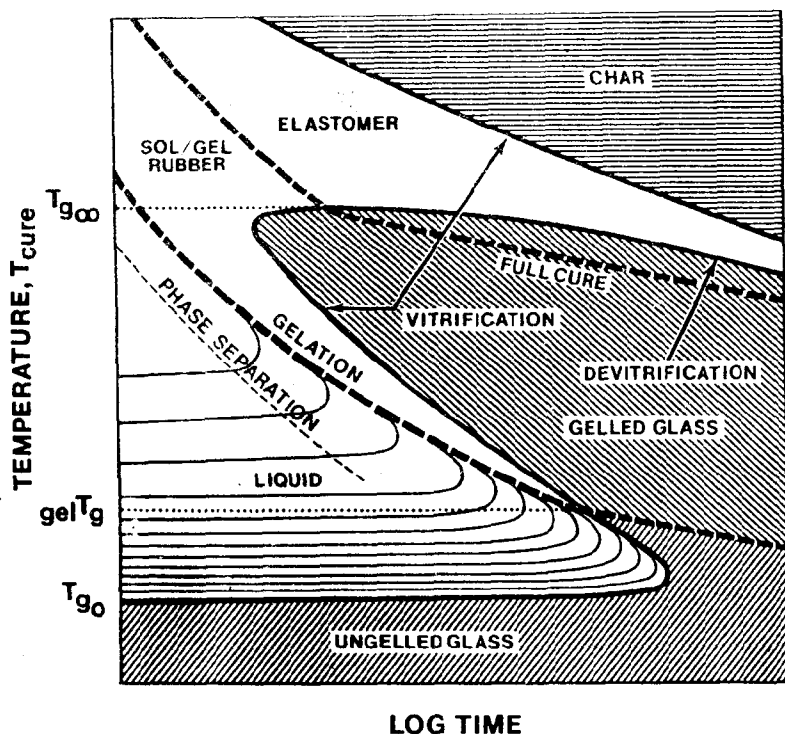


FIG. 1. Time-temperature-transformation (TTT) cure diagram for a reactive thermosetting polymer system showing the different states encountered during isothermal reaction. Such a diagram is useful for designing plastic systems to replace metals. T_{g0} , T_{g_c} and $T_{g\infty}$ are the glass transition temperature of the reactants, the temperature at which the times to gelation and vitrification are the same, and the glass transition temperature of the fully reacted system, respectively. The states are liquid, sol/gel rubber, elastomer, gelled glass, ungelled (or sol) glass, and char. The full cure line (i.e., $T_g = T_{g_c}$) divides the gelled glass region into sol/gel glass and gel (fully cured) glass regions. Successive isoviscous contours shown in the liquid region differ by a factor of ten. The diagram also shows the locus of the onset of phase separation in which a second phase (e.g. rubber) separates during cure: the presence of a dispersed phase modifies the properties of the cured material.

resins, which are used in the technological literature, correspond to sol glass, sol/gel glass and gel glass, respectively. The diagram also displays the critical temperatures T_{g_0} , $_{gel}T_g$, and T_{g_0} which are, respectively, the glass transition temperature of the fully cured system, the temperature at which gelation and vitrification occur simultaneously, and the glass transition temperature of the reactants.

The schematic isothermal TTT cure diagram of Fig. 1 includes a series of isoviscous contours in the liquid region, successive contours differing by a factor of ten.³ Visual extrapolation of the isoviscous contours suggests that the vitrification process below $_{gel}T_g$ is an isoviscous one.

Much of the behavior of thermosetting materials can be understood immediately in terms of the TTT cure diagram through the influence of the gelation, vitrification, and devitrification events on properties: gelation retards macroscopic flow, and retards growth of a dispersed phase (as in rubber-modified systems); vitrification retards chemical conversion; devitrification due to thermal degradation marks the limit in time for the material to support a substantial load. The remainder of this section amplifies these statements:

The ungelled glassy state is the basis of commercial molding materials since, on heating, the ungelled (sol) material can flow before gelling. Formulations can be processed as solids (e.g. molding compositions) when T_{g_0} is above ambient temperature; they can be processed as liquids (e.g. casting fluids) when T_{g_0} is below ambient temperature.

Parameter $_{gel}T_g$ is a critical temperature in determining the upper temperature for storing reactive materials to avoid gelation. The glass transition temperature of the material at the composition corresponding to gelation is $_{gel}T_g$ since at the point of gelation the glass transition temperature has risen to $_{gel}T_g$.

The morphology developed in a two-phase system (e.g. those in which rubber-rich domains precipitate as a dispersed phase) depends on the temperature of cure. The reaction temperature determines the competition between thermodynamic and kinetic (transport) factors. For optimum mechanical properties, a two-phase system will be cured at one temperature to control the morphology, and subsequently cured, usually at higher temperatures, to full cure to complete the reactions of the matrix.

Shrinkage stresses due to cure begin to develop with adhesion to a rigid substrate at gelation above $_{gel}T_g$ and at vitrification below $_{gel}T_g$.

The tensile stresses in the resin and the corresponding compressive stresses on a substrate are important in composite behavior.

Prolonged isothermal cure at T_{cure} below $T_{g\infty}$ would lead to $T_g = T_{\text{cure}}$ if the reactions were quenched by the process of vitrification. In practice $T_g > T_{\text{cure}}$ for three principal reasons: (1) T_g can increase during the heating scan used to measure it; (2) although vitrification is defined to occur when $T_g = T_{\text{cure}}$, T_g as usually measured does not correspond to the glassy state but rather to approximately halfway between the rubbery and glassy states, and so isothermal reactions will proceed beyond the assigned time of vitrification; and (3) reactions do proceed in the glassy state to extents depending on the influence of the glassy state on the reaction mechanism.

Correlations between macroscopic behavior and molecular structure of the reactants result most clearly for fully cured materials. Full cure is attained most readily by reacting above $T_{g\infty}$; it can be achieved more slowly by curing below $T_{g\infty}$ to the full cure line of the TTT cure diagram.

For cure below $_{\text{gel}}T_g$ the cure reactions lead eventually to gelation. At high temperatures other chemical reactions can lead to thermal degradation. Thermal degradation can result in devitrification as the glass transition temperature decreases through the isothermal temperature due to decrease in crosslinking, or due to the formation of low molecular weight plasticizing material. Degradation can also result in vitrification (e.g. char formation) as the glass transition temperature rises to the isothermal temperature due to increase in crosslinking or volatilization of low molecular weight plasticizing materials.⁴ For high- $T_{g\infty}$ systems there is competition between cure and thermal degradation.

The limiting viscosity in the fluid state is controlled by gelation above $_{\text{gel}}T_g$, and by vitrification below $_{\text{gel}}T_g$. At gelation the weight-average molecular weight and zero-shear-rate viscosity become infinite. Viscosity in the vicinity of vitrification is described by the Williams-Landel-Ferry (WLF) equation.¹¹

Recording the time to reach a specified viscosity (Fig. 1) is often used as a practical method for measuring gelation times: above temperature $_{\text{gel}}T_g$ the apparent activation energies obtained from the temperature dependence of the time to reach a specified viscosity approach the true activation energy for the chemical reactions leading to gelation with increase of the specified viscosity.¹

The times to gelation and to vitrification each can be computed from

the reaction kinetics, the conversion at gelation (which is constant according to Flory's theory of gelation),¹² and the conversion at vitrification (which increases with T_{cure}), respectively. Since vitrification occurs when the glass transition temperature rises to the temperature of cure, computation of the time to vitrify requires knowledge of the relationship between T_g and conversion (see Fig. 2, which shows T_g increases with conversion at an increasing rate). In the absence of diffusion control, the general kinetic equation describing the reaction is $dX/dt = A \exp(-E_A/RT)f(X)$ where X is the extent of reaction and the other symbols have their usual meanings. The times to gelation and (in the absence of diffusion control) to vitrification at different temperatures can be computed using this equation, knowledge of X_{gel} (for gelation) and a relationship between X and T_g (for vitrification) (Fig. 2), and the reaction kinetics.^{3,7,13} The influence of diffusion control on the reaction rate can be deduced in principle from the experimentally measured vitrification curve.

The 'S'-shaped vitrification curve obtained experimentally (in the

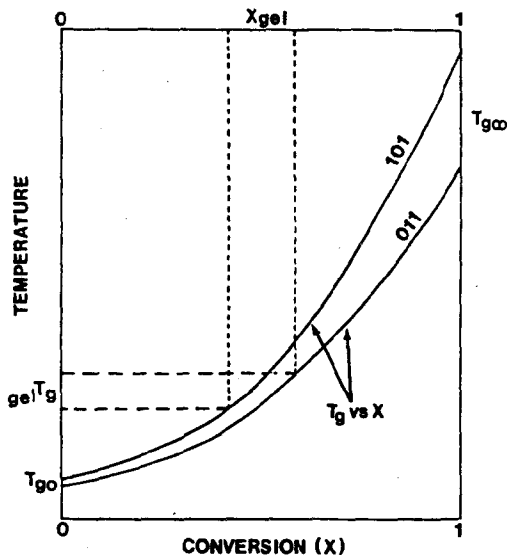


FIG. 2. Schematic diagram of T_g vs conversion at vitrification for reactants differing in functionality ($101 > 011$). The conversions at gelation are also included. The diagram is useful for demonstrating the effect of increasing functionality on gelation, vitrification, and the temperatures $_{\text{gel}}T_g$, T_{g0} , and T_{∞} . (Reproduced with permission from *Journal of Applied Polymer Science*.⁴)

absence of thermal degradation) has been matched computationally for one epoxy system from temperature T_{g_0} to temperature T_{g_∞} .³

The vitrification curve is generally 'S'-shaped for both network- and linear-forming step-growth reactions and for linear chain-growth reactions.⁷ At temperatures immediately above T_{g_0} , the time to vitrification passes through a maximum in consequence of the opposing influences of the temperature dependence of the viscosity and the reaction rate constant. Immediately below T_{g_∞} , the time to vitrification passes through a minimum in consequence of the opposing influences of the temperature dependence of the reaction rate constant and the decreasing concentration of reactive sites at vitrification as T_{g_∞} is approached. Knowledge of the minimum time and the corresponding temperature is economically useful in molding technology where molds can only be opened after solidification.

The conversion at vitrification can be computed in principle by relating the glass transition temperature to contributions from the molecular weight and from the crosslinking density, both of which vary with conversion.^{7,8} For linear polymerization the computation is simplified by the absence of crosslinking.¹⁴

The fractional extent of reaction at vitrification and the time to vitrify, like gelation, decrease with increasing functionality of the reactants.⁴ The effect of increasing functionality on gelation, vitrification, and the temperatures T_{gel} , T_{g_0} , and T_{g_∞} can be understood from consideration of X vs T_g and X_{gel} relationships such as those of Fig. 2.⁴

Increasing cure time at any temperature leads to increasing conversion, T_g , and crosslinking density. Prior to vitrification the modulus and density at the curing temperature also increase. However, on cooling intermittently from the curing temperature to a temperature well below T_g (e.g. room temperature for high- T_g materials), the modulus and density are found to decrease whereas absorption of water is found to increase with increasing extent of cure.⁹ A common basis for these interrelated phenomena is the increasing free volume at room temperature (RT) with increasing extent of cure.^{10,15}

2. TORSIONAL BRAID ANALYSIS/TORSION PENDULUM: A TECHNIQUE FOR CHARACTERIZING THERMOSETTING SYSTEMS

A freely oscillating torsion pendulum can be used in two ways to characterize polymeric systems, namely in the conventional torsion-

pendulum (TP) mode and in the torsional braid analysis (TBA) mode.^{1,2,16-22} Section 3 includes application of the TP/TBA technique to an investigation of the cure and properties of rubber-modified epoxy systems.^{5,6}

Figure 3 shows a schematic diagram of the pendulum, which consists of a specimen held in place with clamps attached to two rods. The upper supporting rod is held vertically in alignment with a 2 in (5 cm) Teflon sleeve and is rigidly attached to a gear. The lower extender rod hangs freely and is magnetically coupled to a polaroid disc at its lower end.

The pendulum is enclosed in an air-tight cylindrical chamber (0.5 in (1.3 cm) diameter), whose atmosphere can be closely controlled and monitored: inert, water-doped, and reactive gases have been used. There are no electronic devices within the specimen chamber. Dry helium, rather than nitrogen, is usually employed as an inert atmosphere because of its higher thermal conductivity at cryogenic temperatures. An on-line electronic hygrometer can be used to continuously monitor the water vapor content of atmospheres from <20 to 20 000 ppm H₂O. A cylindrical copper block, round which cooling coils for liquid nitrogen and band heaters are wound, surrounds the pendulum. Excellent temperature control is achieved by virtue of the large thermal mass of the copper block, with a temperature spread of <1°C over a 2 in (5 cm) specimen. A temperature programmer/controller system permits experiments to be performed in isothermal ($\pm 0.1^\circ\text{C}$ above 30°C) and dynamic modes from -190 to 400°C ; in the dynamic mode the temperature may be increased or decreased linearly at rates of 0.05 – $5^\circ\text{C}/\text{min}$. Cooling is achieved by controlling the flow of liquid nitrogen from a pressurized container. Routine temperature scans are made at rates of change of temperature of $\pm 1.5^\circ\text{C}/\text{min}$. Measurements have been made as low as 4K and as high as 700°C in modified apparatus.

A key factor in the instrumentation is the non-drag optical transducer which produces an electrical response that varies linearly with angular displacement. A polarizing disc is used as part of the inertial member of the pendulum, and a stationary second polarizer is positioned in front of a linearly-responding photo-cell. An analog electrical signal is obtained from a light beam passing through the pair of polarizers.

The clamps on the pendulum allow a variety of specimens to be used: film, fiber, or coating on glass braid or foil substrate. Depending on the specimen, the system can be used as a conventional torsion

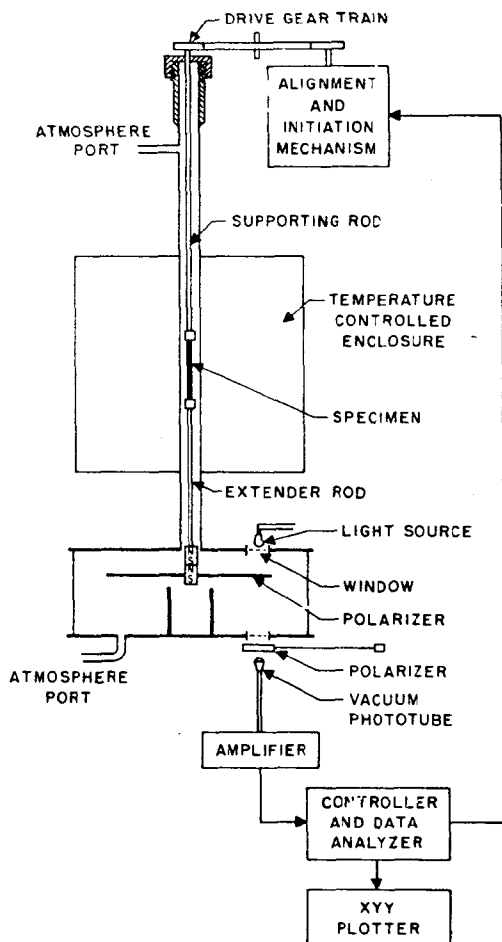


FIG. 3. Schematic diagram of automated torsion pendulum and TBA instrument. An analog electrical signal results from using a light beam passing through a pair of polarizers, one of which oscillates with the specimen. The pendulum is aligned for linear response of the transducer and oscillations are initiated using a gear train controlled by a computer. The computer also processes the damped waves to provide the elastic modulus and mechanical damping data, which are plotted against temperature or time.